Metastable configurations on the Bethe lattice

A. Pagnani
Dipartimento di Fisica, SMC, INFM, Università degli Studi di Roma "La Sapienza," Piazzale Aldo Moro 2, I-00185 Roma, Italy

G. Parisi
Dipartimento di Fisica, SMC, INFM, and INFN, Università degli Studi di Roma "La Sapienza," Piazzale Aldo Moro 2, I-00185 Roma, Italy

M. Ratiéville
Dipartimento di Fisica, SMC, INFM, Università degli Studi di Roma "La Sapienza," Piazzale Aldo Moro 2, I-00185 Roma, Italy and Laboratoire de Physique Théorique et Modèles Statistiques, Université Paris-Sud, 91405 Orsay, France
(Received 14 October 2002; published 19 February 2003)

We present a general analytic method to compute the number of metastable configurations as a function of the energy for a system of interacting Ising spins on the Bethe lattice. Our approach is based on the cavity method. We apply it to the case of ferromagnetic interactions, and also to the binary and Gaussian spin glasses. Most of our results are obtained within the replica symmetric ansatz, but we illustrate how replica symmetry breaking can be performed.

DOI: 10.1103/PhysRevE.67.026116 PACS number(s): 05.50.+q, 75.50.Lk

I. INTRODUCTION

Despite years of efforts, the nature of the glassy phase of finite-dimensional spin glasses is still not clear. It is still debated whether the replica symmetry breaking (RSB) scheme proposed by Parisi to solve the mean field fully connected Sherrington-Kirkpatrick model (SK), and implying the existence of an exponentially large number of pure states with an ultrametric structure, holds in some way for these systems. Part of the difficulty to settle the question is the very poor analytical tractability of finite-dimensional systems.

Looking for more realistic—but still tractable—models than SK, much attention was recently paid to spin glasses on random graphs of finite connectivity. These models incorporate the short range nature of interactions, but without the underlying geometry of the finite-dimensional models. It has been shown that the replica symmetric (RS) solution of spin glasses on random graphs of finite connectivity is unstable at low temperature [1,2]. Unfortunately, working out the RSB scheme is far more difficult than for the SK because the glassy phase can no longer be characterized by the only two-spin overlap $\langle \sigma_a \sigma_b \rangle$ between two distinct replicas a and b, but requires all of the multispin overlaps. Recently, a different approach was suggested in Ref. [3], based on the cavity method and population algorithms, that allows for a numerical solution at the level of one step RSB (1RSB). The method can be virtually extended to any step of RSB, at the price of increasing computer resources.

In this paper, we use similar ideas to shed a new light onto an old problem: the computation of the number of metastable configurations. A configuration is said to be metastable if its energy cannot be decreased by flipping a single spin. One expects, within the RSB scenario, that a consequence at zero temperature of the exponential number of pure states is an exponential number of metastable configurations. Note, however, that these two concepts are not as obviously linked as it might seem: in systems with finite connectivity, the zero temperature limit of the pure states are not the metastable configurations, but are argued to be the configurations stable with respect to an arbitrary finite number of spin flips [4,5].

Let us call configurational entropy $S_C(E)$ the logarithm, divided by the number of spins, of the number of metastable configurations having an energy density equal to E. Lots of efforts have been devoted to the study of S_C for SK. More recently, attention turned to spin systems on random graphs. On random graphs with fixed finite connectivity, annealed computations were carried out for the binary spin glass [6], and the ferromagnet was addressed in Ref. [7]. On random graphs of fluctuating finite connectivity, the case of the ferromagnet was solved in Ref. [9]—also *via* a population algorithm, but in a different context as ours—and the authors give hints how to address the quenched computation of spin glasses.

Our method, which is quite general, enables us to recover all the above results. As contributions, we carry out quenched computations in the case of the Gaussian or binary spin glass on random graphs of fixed finite connectivity, and we exemplify the implementation of 1RSB.

In the following, we stick to the case of random graphs of fixed finite connectivity. For the sake of concision, we display no result about the fluctuating connectivity, but it is easy to generalize our method to this case.

The layout of the paper is the following. In Sec. II, we give several definitions and we set the notations. In Sec. III, we derive our basic equations in the RS framework. In Sec. IV, we analytically solve these equations in the case of a ferromagnet. We compare our results with the microcanonical approach of Ref. [7]. In Sec. V, we turn to the binary spin glass, where the coupling constants are ± 1. The population algorithm shows up there. In Sec. VI, we address the slightly more involved Gaussian spin glass. Eventually, in Sec. VII, we show how to perform 1RSB, and illustrate the algorithm on the case of the spin glass with binary couplings.

II. THE SYSTEM UNDER STUDY

Following Ref. [3], we call the Bethe lattice a random graph with fixed connectivity equal to $k+1$, i.e., the number

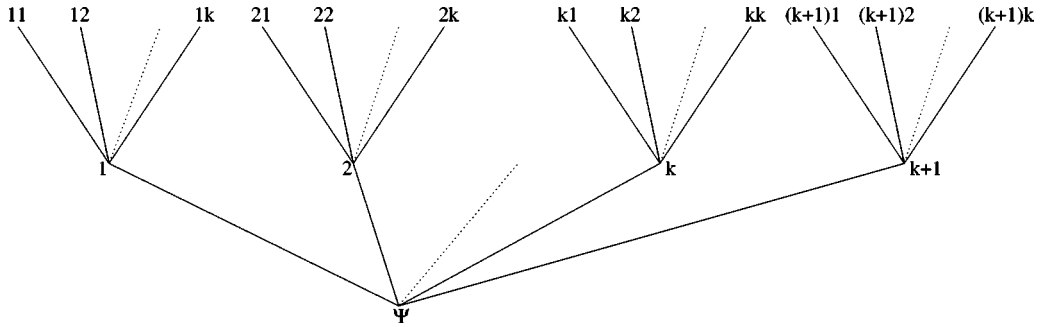

FIG. 1. Part of a Cayley tree.

of edges incident to each vertex is exactly $k+1$. Locally, such a graph has the structure of a Cayley tree, and can be obtained with the following procedure: starting from a root (or ancestor) Ψ, one builds the first generation of $k+1$ sons, and then successive generations of k sons to each vertex, as displayed in Fig. 1. By contrast to the Cayley tree, the Bethe lattice has loops, but small ones are rare: the typical length of a loop is of order $\ln N$. In a practical case, one uses the treelike structure to write down recursive (or cavity in the language of the physics of disordered systems [10]) equations, and the existence of loops is enforced by saying that all the spins are equivalent, which is not true for the Cayley tree (in particular, the Cayley tree has strong boundary effects).

On each vertex A of the Bethe lattice stands a spin, and these spins interact through the Hamiltonian

$$\mathcal{H}=-\sum_{\{A,B\}} J_{A,B}\sigma_A\sigma_B, \tag{1}$$

where the sum runs over all the edges. The coupling constants $J_{A,B}$ may be fixed, as in the case of the ferromagnet, or they may be quenched random variables in the case of a spin glass.

The local field acting on the spin A is $H_A=\Sigma_{B\in\mathcal{V}(A)}J_{A,B}\sigma_B$, where the sum runs over the $k+1$ first neighbors of A. The metastable states are characterized by $\forall A, H_A\sigma_A\geqslant 0$. Our aim is to compute the partition function restricted to the metastable configurations:

$$Z=\mathrm{Tr}\left[e^{-\beta\mathcal{H}}\prod_A \Theta(H_A\sigma_A)\right], \tag{2}$$

where Θ is the heaviside step function such that $\Theta(u)=1$ if $u\geqslant 0$, 0 otherwise, and Tr stands for the summation over all the possible values of all the spins.

III. THE CAVITY EQUATIONS

Let us introduce, in close analogy with the construction of the *infinite tree* in Ref. [11], a simple labeling rule for the vertices of a tree: the sons of the root are labeled 1,2, . . . ,k. Then recursively the sons of a vertex labeled $(i_1\cdots i_p)$ are labeled $(i_1\cdots i_p 1), \ldots (i_1\cdots i_p k)$. If $A=(i_1\cdots i_p)$, we can define the *norm* of the symbol as $|A|\equiv p$.

The basic building block of the cavity solution is a branch of the Cayley tree, i.e., a subtree made of a given vertex different from the root and all its descendants. In Fig. 2 is drawn a branch rooted at Φ. Let us call it T_Φ.

The key property of a branch is that it is structurally similar to each of its sub-branches made of a given vertex and all its descendants. This makes a recursive approach possible to study the thermodynamics of a branch. We will see afterwards how to use the results for the Bethe lattice.

A. Computing the metastable states on a branch

As it will be clear later, on a branch it is convenient to require that all the spins are stables, except the root. The Hamiltonian of a branch is

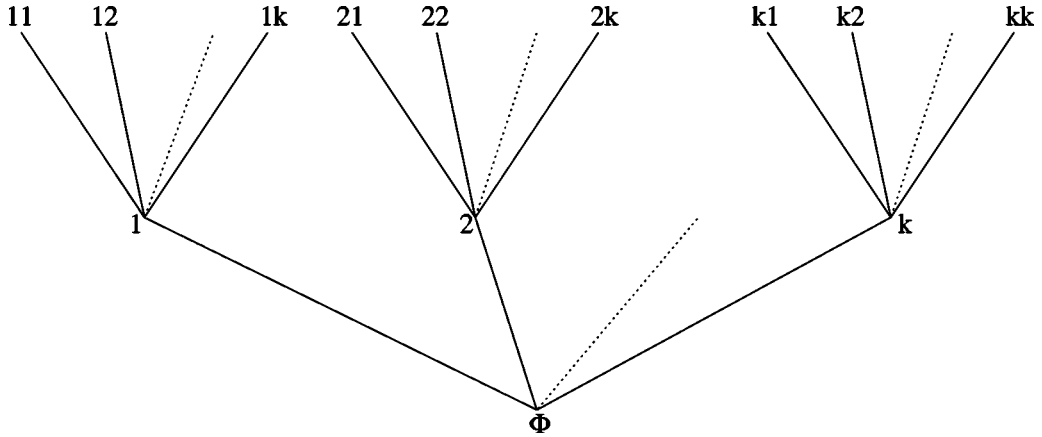

FIG. 2. A branch.

$$\mathcal{H}_\Phi = -\sum_{\{A,B\}\in T_\Phi} J_{A,B}\sigma_A\sigma_B . \tag{3}$$

The definition of the partition function is

$$Z_\Phi = \mathrm{Tr}\left[e^{-\beta\mathcal{H}_\Phi} \prod_{A\in T_\Phi\setminus\Phi} \Theta(H_A\sigma_A)\right]. \tag{4}$$

By contrast to all the other spins in T_Φ, which have $k+1$ neighbors, spin Φ lacks one neighbor. In all the following, the local field acting on such a spin with only k neighbors will be called a cavity field and denoted by a small h (here h_Φ). We call $p_\Phi(h,\sigma)$ the joint density probability of h_Φ and the value of spin Φ. One has

$$p_\Phi(h,\sigma) = \frac{1}{Z_\Phi}\mathrm{Tr}\left[e^{-\beta\mathcal{H}_\Phi}\delta(\sigma_\Phi-\sigma) \times \prod_{|A|\geqslant 1}\Theta(H_A\sigma_A)\,\delta(h_\Phi - h)\right]. \tag{5}$$

We call $T_1,\ldots,T_k$ the subtrees of T_Φ engendered by points $1,\ldots,k$. We can define their Hamiltonians similarly to Eq. (3), and write

$$\mathcal{H}_\Phi = \sum_{i=1}^{k}\mathcal{H}_i - h_\Phi\sigma_\Phi . \tag{6}$$

Splitting the trace, Eq. (5) can be restated as

$$p_\Phi(h,\sigma) = \frac{1}{Z_\Phi}e^{\beta h\sigma}\mathop{\mathrm{Tr}}_{\sigma_1,\ldots,\sigma_k}\delta(h_\Phi-h)\mathop{\mathrm{Tr}}_{|A|\geqslant 2} e^{-\beta\Sigma_{i=1}^{k}\mathcal{H}_i} \times\prod_{i=1}^{k}\Theta(H_i\sigma_i)\prod_{|A|\geqslant 2}\Theta(H_A\sigma_A). \tag{7}$$

Now separate H_i into two contributions

$$H_i = \sum_{j=1}^{k} J_{i,ij}\sigma_{ij} + J_{\Phi,i}\sigma_\Phi , \tag{8}$$

and enforce the fact that the first one is the cavity field acting on spin i in the absence of Φ through the identities

$$1 = \int dh_i\,\delta\left(\sum_j J_{i,ij}\sigma_{ij} - h_i\right). \tag{9}$$

Plugging Eqs. (8) and (9) into Eq. (7), one gets

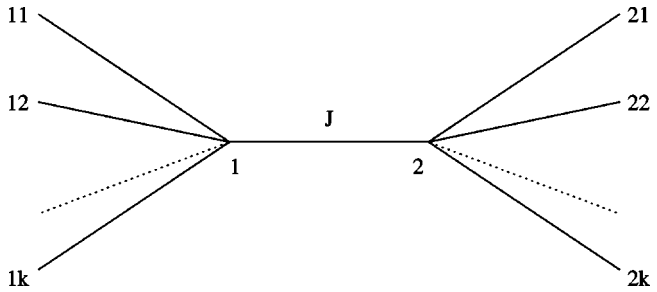

FIG. 3. Result of the merging (M2) of two branches.

$$p_\Phi(h,\sigma) = \frac{1}{Z_\Phi}e^{\beta h\sigma}\mathop{\mathrm{Tr}}_{\sigma_1,\ldots,\sigma_k}\delta(h_\Phi-h)\prod_{i=1}^{k}\int dh_i\Theta[(h_i + J_{\Phi,i}\sigma)\sigma_i]\mathop{\mathrm{Tr}}_{|A|\geqslant 2} e^{-\beta\Sigma_{i=1}^{k}\mathcal{H}_i}\prod_{|A|\geqslant 2}\Theta(H_A\sigma_A) \times\prod_{i=1}^{k}\delta\left(\sum_j J_{i,ij}\sigma_{ij} - h_i\right). \tag{10}$$

Comparing to Eq. (5), it turns out that the second line in the above equation is nothing but the product of $Z_i p_i(h_i,\sigma_i)$ for $i=1,\ldots,k$. So one eventually obtains the following recursion relation:

$$p_\Phi(h,\sigma) = \frac{Z_1\cdots Z_k}{Z_\Phi}e^{\beta h\sigma}\mathop{\mathrm{Tr}}_{\sigma_1,\ldots,\sigma_k}\delta(h_\Phi-h)\prod_{i=1}^{k} \times\int dh_i\Theta[(h_i+J_{\Phi,i}\sigma)\sigma_i]p_i(h_i,\sigma_i). \tag{11}$$

By averaging over the coupling constants and the random graphs (operation denoted by $\overline{\cdots}$), one defines the probability distributions $\mathcal{P}_\Phi^{(h,\sigma)}(p) = \overline{\delta(p_\Phi(h,\sigma)-p)}$ Equation (11) induces a functional relation between $\mathcal{P}_\Phi^{(h,\sigma)}$ and the analogous probability distributions $\mathcal{P}_i^{(h,\sigma)}$ for $i=1,\ldots,k$. In the Bethe lattice, all spins are required to be equivalent so we impose the condition

$$\forall i,\quad \mathcal{P}_\Phi = \mathcal{P}_i = \mathcal{P}. \tag{12}$$

This yields a self-consistency equation for $\mathcal{P}$.

B. Performing measures on the Bethe lattice

Having solved the thermodynamics of a branch, the idea of Ref. [3] is to describe the Bethe lattice as the result of the merging of several branches. We define two merging procedures.

(M1) Take $k+1$ branches, with roots labeled $i=1,\ldots,k$ and merge them onto a new spin Ψ. The resulting tree is the one of Fig. 1.

(M2) Take two branches, with roots labeled 1 and 2, and merge them *via* a new bond of coupling constant J, without adding any site. See Fig. 3.

Operation (M1) is very similar to the iteration Eq. (11): the differences are that k is to be substituted by $k+1$, and one must enforce the stability of the spin Ψ. After the merging, the joint density probability of the value of spin Ψ and the local field H_Ψ acting on it is $P_\Psi(H,\sigma)$, given by

$$P_\Psi(H,\sigma)=\frac{Z_1\cdots Z_{k+1}}{Z}e^{\beta H\sigma}\Theta(H\sigma)\operatorname*{Tr}_{\sigma_1,\ldots,\sigma_{k+1}}\delta(H_\Psi - H)\prod_{i=1}^{k+1}\int dh_i\Theta[(h_i+J_{\Psi,i}\sigma)\sigma_i]p_i(h_i,\sigma_i). \tag{13}$$

Summing over all the possible (H,σ) and taking the logarithm, one gets the variation of the free energy of the system during the merging

$$\Delta F_1=-\frac{1}{\beta}\ln\left[\sum_\sigma\int dH e^{\beta H\sigma}\Theta(H\sigma)\operatorname*{Tr}_{\sigma_1,\ldots,\sigma_{k+1}}\delta(H_\Psi - H)\prod_{i=1}^{k+1}\int dh_i\Theta[(h_i+J_{\Psi,i}\sigma)\sigma_i]p_i(h_i,\sigma_i)\right]$$
$$=-\frac{1}{\beta}\ln\left[\operatorname*{Tr}_{\sigma,\sigma_1,\ldots,\sigma_{k+1}}e^{\beta H_\Psi\sigma}\Theta(H_\Psi\sigma)\times\prod_{i=1}^{k+1}\int dh_i\Theta[(h_i+J_{\Psi,i}\sigma)\sigma_i]p_i(h_i,\sigma_i)\right]. \tag{14}$$

As far as operation (M2) is concerned, it is straightforward to derive the variation of the free energy

$$\Delta F_2=-\frac{1}{\beta}\ln\left[\operatorname*{Tr}_{\sigma_1,\sigma_2}e^{\beta J\sigma_1\sigma_2}\int dh_1dh_2\Theta[(h_1+J\sigma_2)\sigma_1]\times\Theta[(h_2+J\sigma_1)\sigma_2]p_1(h_1,\sigma_1)p_2(h_2,\sigma_2)\right]. \tag{15}$$

One can easily deduce the density of free energy F of the Bethe lattice from ΔF_1 and ΔF_2. Assuming that each branch has a number of spins equal to N, the system after the merging (M1) has $N(k+1)+1$ spins, and its free energy can by written in two ways:

$$[N(k+1)+1]F=(k+1)F_{branch}+\overline{\Delta F_1}, \tag{16}$$

where F_{branch} is the free energy of one of the branches before the merging. For operation (M2), one has

$$(2N)F=2F_{branch}+\overline{\Delta F_2}. \tag{17}$$

Elimination of F_{branch} between the above equations yields

$$F=\overline{\Delta F_1}-\frac{k+1}{2}\overline{\Delta F_2}. \tag{18}$$

Note that the above derivation holds for any extensive and self-averaging observable. Thus, the density of energy E of the Bethe lattice is

$$E=\overline{\Delta E_1}-\frac{k+1}{2}\overline{\Delta E_2}, \tag{19}$$

where ΔE_1, resp. ΔE_2, is the variation of energy under the merging process (M1), respectively (M2):

$$\Delta E_1=-\sum_\sigma\int dH P_\Psi(H,\sigma)H\sigma=-\frac{\operatorname*{Tr}_{\sigma,\sigma_1,\ldots,\sigma_{k+1}}H_\Psi\sigma e^{\beta H_\Psi\sigma}\Theta(H_\Psi\sigma)\prod_{i=1}^{k+1}\int dh_i\Theta[(h_i+J_{\Psi,i}\sigma)\sigma_i]p_i(h_i,\sigma_i)}{\operatorname*{Tr}_{\sigma,\sigma_1,\ldots,\sigma_{k+1}}e^{\beta H_\Psi\sigma}\Theta(H_\Psi\sigma)\prod_{i=1}^{k+1}\int dh_i\Theta[(h_i+J_{\Psi,i}\sigma)\sigma_i]p_i(h_i,\sigma_i)}, \tag{20}$$

and

$$\Delta E_2=-J\frac{\operatorname*{Tr}_{\sigma_1,\sigma_2}\sigma_1\sigma_2e^{\beta J\sigma_1\sigma_2}\int dh_1dh_2\Theta[(h_1+J\sigma_2)\sigma_1]\Theta[(h_2+J\sigma_1)\sigma_2]p_1(h_1,\sigma_1)p_2(h_2,\sigma_2)}{\operatorname*{Tr}_{\sigma_1,\sigma_2}e^{\beta J\sigma_1\sigma_2}\int dh_1dh_2\Theta[(h_1+J\sigma_2)\sigma_1]\Theta[(h_2+J\sigma_1)\sigma_2]p_1(h_1,\sigma_1)p_2(h_2,\sigma_2)}. \tag{21}$$

These results can be applied to a wide variety of models: up to now we have not specified the coupling constants.

IV. THE FERROMAGNETIC CASE: AN EXACTLY SOLVABLE MODEL

First, we concentrate on a simple case where all the above equations can be worked out analytically. The previous formalism allows for the computation of the metastable states of the $k=2$ Ising ferromagnet. When the couplings all have the same absolute value $|J|=1$, the cavity field can take only value in the set $(-2,0,2)$. Thus, integration with respect to the h_i in Eq. (11) and other formulas reduces to a finite summation. Moreover, in the case of the Ising ferromagnet (i.e., $J=1$) the system is homogeneous, therefore the cavity equations should not depend on the site index and we can define the joint probabilities $p_0=p(h=-2,\sigma=-1)$, $p_1=p(h=-2,\sigma=1)$, $p_2=p(h=0,\sigma=-1)$, $\ldots$, $p_5=p(h=2,\sigma=1)$ of Eq. (11) identically for all the lattice sites. A simple enumeration shows that Eq. (11) reduces to the following system of equations:

$$\begin{gathered} cp_0e^{2\beta}=p_1^2, \quad cp_1e^{-2\beta}=p_1^2+2p_1p_3+p_3^2, \\ cp_2=2p_1p_2+2p_1p_4, \\ cp_3=2p_1p_4+2p_3p_4, \quad cp_4e^{-2\beta}=p_2^2+2p_2p_4+p_4^2, \\ cp_5e^{2\beta}=p_4^2, \end{gathered} \tag{22}$$

together with the normalization condition $\Sigma_{i=0}^{5}p_i=1$. The symmetries of the system fix some conditions on the values of p_i. The relations $p_0=p_5$, $p_1=p_4$, $p_2=p_3$ hold in the paramagnetic phase (PA). If the overall Z_2 symmetry is spontaneously broken the system encounters a ferromagnetic (FM) phase characterized by $p_2=p_3=p_4=p_5=0$ (obviously there is also the solution with the opposite magnetization, for which $p_0=p_1=p_2=p_3=0$). In the FM case the solution is given by

$$p_0=\frac{1}{1+e^{4\beta}}, \quad p_1=\frac{1}{1+e^{-4\beta}}, \quad c=\frac{1}{e^{-2\beta}+e^{-6\beta}}. \tag{23}$$

The solution in the PA case is slightly more involved

$$\begin{gathered} p_0=\frac{cD^4}{64x^5}, \quad p_1=\frac{cD^2}{4x}, \quad p_2=\frac{cD^3}{8x^3}, \\ c=\frac{1}{2}\left[\frac{D^4}{64x^5}+\frac{D^3}{8x^3}+\frac{D^2}{4x}\right]^{-1}, \end{gathered} \tag{24}$$

where $x=(e^{2\beta}/4)^{1/3}$ and $D=\sqrt{x^4+2x}-x^2$. The problem of the iterative stability of both the FM and PA solutions can be addressed studying the spectrum of the Jacobian of the system of equations (22). It turns out that the PA solution becomes unstable below a $T_c^{PA}=\ln^{-1}(2\sqrt{\frac{2}{3}})=2.039\,091$ and the FM one above $T_c^{FM}=2\ln(2)=2.885\,390$. Once we have calculated the cavity fields, we can measure the thermodynamic potential using the merging procedures explained in the proceding section.

Let us consider first the FM solution

$$\begin{gathered} \Delta E_1=-3, \quad \Delta F_1=-3\left[1-\frac{1}{\beta}\ln(1+e^{-4\beta})\right], \\ \Delta E_2=-1, \quad \Delta F_2=\frac{2}{\beta}\ln(1+e^{-4\beta})-1. \end{gathered} \tag{25}$$

Inserting Eq. (25) into Eqs. (18) and (19), we readily obtain $E=F=-\frac{3}{2}$, i.e., the system is completely frozen in its ground state.

The PA solution is worked analogously.

$$\begin{gathered} \Delta E_1=-\frac{N_1}{D_1}, \quad \Delta F_1=-\frac{1}{\beta}\ln(D_1), \\ \Delta E_2=-\frac{N_2}{D_2}, \quad \Delta F_2=-\frac{1}{\beta}\ln(D_2), \end{gathered} \tag{26}$$

where

$$\begin{aligned} N_1&=2p_1^3(3e^{\beta}+e^{3\beta})+6p_1^2p_2(e^{3\beta}+2e^{\beta}) \\ &\quad +6p_1p_2^2(e^{\beta}+e^{3\beta}), \\ D_1&=6p_1^3(e^{\beta}+e^{3\beta})+6p_1^2p_2(3e^{3\beta}+2e^{\beta}) \\ &\quad +6p_1p_2^2(e^{\beta}+3e^{3\beta})+6p_2^3e^{3\beta}, \\ N_2&=2p_1^2e^{-\beta}-2(p_1+p_2)^2e^{\beta}, \\ D_2&=2p_1^2e^{-\beta}+2(p_1+p_2)^2e^{\beta}, \end{aligned} \tag{27}$$

and for the p_i we use Eq. (24). In Fig. 4, we display both energy and free energy as a function of the temperature. Starting in the low temperature phase, the system gets trapped in the ferromagnetic solution in which all the spins are aligned. This solution is locally stable for the iteration [Eq. (22)] up to temperature T_c^{FM}. We define $T_c=2.228\,512$ as the temperature at which PA and FM solutions have the same energy. Exactly at this temperature, we have the coexistence of the two phases of the system. Above Tc, the PA solution acquires a lower free energy. In Fig. 5, we display the configurational entropy $S_C(E)$ as a function of the energy E. The thin straight line is tangent to the curve exactly at $S_C(E_c)$, where $E_c\equiv E(T_c)=-1.056\,13$, while the dotted curve beneath the tangent is the result of the microcanonical computation of Lefévre and Dean presented in Ref. [7]. Note that the microcanonical branch cannot be obtained in our canonical scheme.

V. THE BINARY SPIN GLASS

Let us now turn to a slightly more complicated case, the binary spin glass, where the coupling constants are quenched

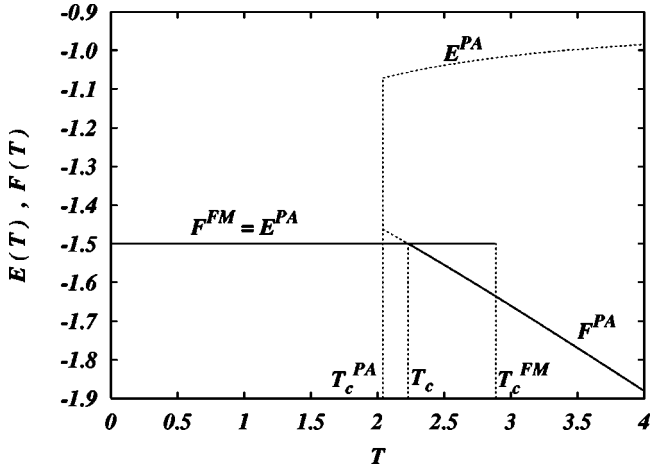

FIG. 4. Thermodynamic potentials E and F vs T for the ferromagnet in the case $k=2$.

independent identically distributed (iid) random variables with the following law:

$$\lambda(J)=\frac{1}{2}[\,\delta(J-1)+\delta(J+1)\,]. \tag{28}$$

As in the above section, an important simplification occurs: the local field acting on a spin can have only a finite number of values. The cavity fields can have $k+1$ values: $-k,-k+2,\ldots,k$, whereas the local field acting on a site with $k+1$ first neighbors can have $(k+2)$ values: $-k-1,-k+1,\ldots,k+1$. But by contrast to the ferromagnet, the system is no longer homogeneous, and the self-consistency equation (12) is a tricky object. To tackle a similar equation, in Ref. [3] is suggested a numerical solution *via* a population algorithm. The basic idea is that a probability distribution can be represented by a large collection of iid random variables distributed according to it.

In our case, the algorithm works as follows: we use a large population of $\mathcal{N}$ sites $i=1,\ldots,\mathcal{N}$, each of which is characterized by a finite set of $2(k+1)$ numbers, the $p_i(h,\sigma)$. After random initialization, one iterates the following sequence:

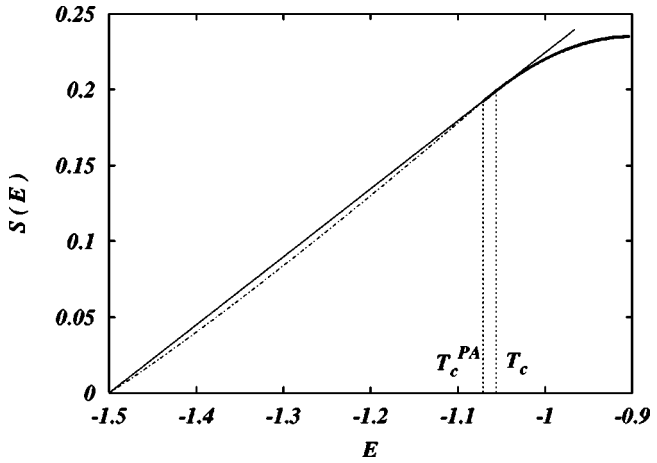

FIG. 5. Configurational entropy S_C vs E for the ferromagnet in the case $k=2$ (see text).

1. Algorithm I

(i) Select $k+2$ sites $i_1,\ldots,i_{k+2}$ at random, and extract some couplings $J_1,\ldots,J_{k+1}$.

(ii) Perform the merging (M1) of the branches rooted at $i_1,\ldots,i_{k+1}$ onto the site $\Psi=i_{k+2}$, that is, compute ΔF_1 with Eq. (14), ΔE_1 with Eq. (20).

(iii) Perform the merging (M2) of the branches rooted at i_1 and i_2, that is compute ΔF_2 with Eq. (15), ΔE_2 with Eq. (21), using for instance the coupling J_1.

(iv) Update the population: perform the merging of the branches rooted at $i_1,\ldots,i_k$ onto the site $\Phi=i_{k+2}$, that is substitute $p_{k+2}(h,\sigma)$ by the result of Eq. (11).

The algorithm converges in a stochastic sense: after a sufficient number of iterations, the $p_i(h,\sigma)$ are distributed according to $\mathcal{P}$. So one can compute the average of the thermodynamic quantities with respect to the couplings by time averaging of the measures performed in steps (ii) and (iii).

In the practical implementation of the algorithm, we have scanned values of $\mathcal{N}$ ranging from 200 to 4000. A careful finite size scaling analysis shows that results are really mildly dependent on $\mathcal{N}$ as soon as $\mathcal{N}>1000$, and the asymptotic extrapolation is always compatible, within statistical errors, with the biggest size we have simulated. The errors are calculated with standard binning procedure, discarding the first half of the simulation. In this way we have a complete control on the *thermalization* of the algorithm. Most of the simulations have been performed also for the same system removing the stability condition on the local fields. We will always refer to these data as AC (all configurations) to distinguish them from the metastable (MS) set of data. For most of the simulations we have performed from $10^3\times\mathcal{N}$ up to $10^4\times\mathcal{N}$ iterations of Algorithm I, which we have verified to be enough both for thermalization and numerical accuracy.

The configurational entropy S_C is the MS entropy.

One should also note that in the case of the Bethe lattice, the choice of the distribution [Eq. (28)] is not crucial and the same results hold in the case of a distribution $\lambda(J)=p\,\delta(J-1)+(1-p)\,\delta(J+1)$ regardless of how small p is and even in the limiting case of a purely antiferromagnetic system. This observation allows for the analytic computation of the critical temperature and the critical energy of this model. Following the route specified in Sec. IV, we calculated the equivalent of the system of equations (22) for purely antiferromagnetic couplings. The stability analysis of the paramagnetic solution gives the same temperature of the FM case, i.e., $T_c=\ln^{-1}(2\sqrt{\frac{2}{3}})$ and $E_c\equiv E(T_c)=-15/14\approx-1.071\,429$. Below this temperature (energy) the replica symmetry is spontaneously broken.

In Fig. 6, we display the logarithm of the number of metastable states as a function of the energy. In the inset we magnify the results for the lowest energies. It is interesting to note that in the region $E<-1.22$, both AC and MS entropies seem to behave linearly on E, and a linear fit works really well. The two curves meet at $E=-1.273(5)$ and $S=0.0172(5)$. This energy is clearly compatible with the replica symmetric value of the ground state $E_0^{RS}=-23/18=-1.277\,777$ [12]. We have an excess of entropy at E_0^{RS}

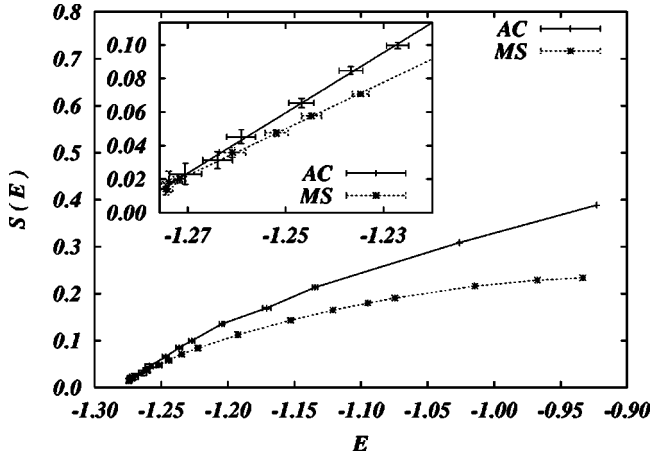

FIG. 6. Entropy vs E for the binary spin glass in the case $k=2$. Inset: magnification of the low-energy region. MC with AC without one spin-flip stability condition.

which is proportional to the density of spins with zero local field in the ground state—such a spin can be flipped without changing the energy. Note that numerical simulations [13] find an entropy of the ground state $S=0.010(1)$, not that far from our RS prediction. As far as the ground state energy is concerned, these simulations give $E=-1.2719(5)$, which is compatible with the result of a 1RSB computation $E\sim -1.2717$ [4]. Therefore, quantitative effects of RSB on this model are rather small, and RSB beyond the second order is expected to yield small corrections.

In Fig. 7, we compare our data with the annealed approximation presented in Ref. [7], while in inset, we magnify the difference $S_{ann}(E)-S(E)$ in the region $E<E_c$. Above this value the annealed approximation is believed to be exact, and in fact our data fall on the analytic curve within the error bars, while below E_c, the two curves split. It is interesting to note that the splitting, barely visible in the main panel for $E>-1.2$, seems to be exponential, at least near E_c (note the logarithmic scale on the y axis of inset).

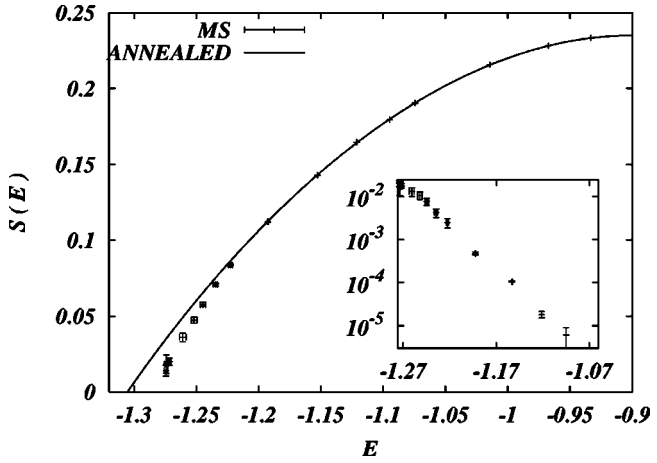

FIG. 7. Entropy vs E for the binary spin glass in the case $k=2$: comparison of the quenched and annealed results. Inset: enlargement of the difference between the annealed and metastable (MS) entropy.

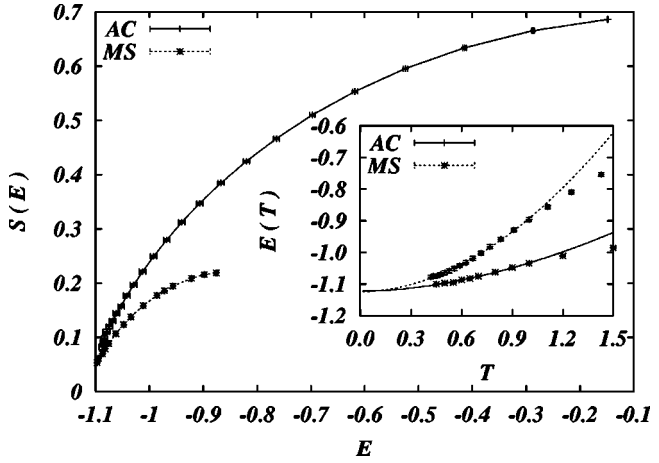

FIG. 8. Entropy vs E for the Gaussian spin glass. Inset: energy vs $T\equiv 1/\beta$. Lines are power-law fits of the low-T region. Note that both curves extrapolate at $T=0$ to the same value (see text).

Let us stress here that it is straightforward to adapt the algorithm to the case of random graphs of fluctuating connectivity of finite mean c. In such a graph, given two points, there is an edge connecting them with probability c/N, and no edge with probability $1-c/N$. Thus, the number of first neighbors of a given site is a random variable distributed according to a Poisson law of mean c. To implement this, one must extract the number $k+1$ according to this law in step (i). The rest is unchanged, except the important fact that step (iv) is no longer to be performed with k branches, but with $k+1$ branches, like step (ii) and that the $k+1$ term in Eqs. (18) and (19) should be replaced by c [8].

VI. THE GAUSSIAN SPIN GLASS

Our method can tackle even more complicated cases, such as the Gaussian spin glass, in which the coupling constants are quenched iid random variables whose law is a Gaussian with unit variance and zero mean.

The local fields are now continuous variables. We choose to represent the probability distribution $p_i(h,\sigma)$ on a site by a large population of $\mathcal{L}$ couples (h,σ) distributed according to p_i.

So on each site $i=1,\ldots,\mathcal{N}$, we have a population $(h_i^\nu,\sigma_i^\nu),\nu=1,\ldots,\mathcal{L}$. The algorithm's layout is similar to Algorithm I.

1. Algorithm II

(i) Select $k+2$ sites $i_1,\ldots,i_{k+2}$ at random, and extract some couplings $J_1,\ldots,J_{k+1}$.

(ii) Perform the merging of the branches rooted at $i_1,\ldots,i_{k+1}$ onto the site $\Psi=i_{k+2}$. In the context of this algorithm, Eqs. (14) and (20) become

$$\Delta F_1=-\frac{1}{\beta}\ln\left[\sum_{\nu=1}^{\mathcal{L}}\sum_{\sigma=\pm 1}e^{\beta H_\Psi^\nu\sigma}\Theta(H_\Psi^\nu\sigma)\times\prod_{j=1}^{k+1}\Theta[(h_{i_j}^\nu+J_j\sigma)\sigma_{i_j}^\nu]\right], \tag{29}$$

$$\Delta E_1 = -\frac{\sum_{\nu=1}^{\mathcal{L}} \sum_{\sigma=\pm 1} H_\Psi \sigma e^{\beta H_\Psi^\nu \sigma} \Theta(H_\Psi^\nu \sigma) \prod_{j=1}^{k+1} \Theta[(h_{i_j}^\nu + J_j\sigma)\sigma_{i_j}^\nu]}{\sum_{\nu=1}^{\mathcal{L}} \sum_{\sigma=\pm 1} e^{\beta H_\Psi^\nu \sigma} \Theta(H_\Psi^\nu \sigma) \prod_{j=1}^{k+1} \Theta[(h_{i_j}^\nu + J_j\sigma)\sigma_{i_j}^\nu]}, \tag{30}$$

$$\text{where} \quad H_\Psi^\nu = \sum_{j=1}^{k+1} J_j \sigma_{i_j}.$$

(iii) Perform the merging of the branches rooted at i_1 and i_2, using for instance the coupling J_1. The formulas (15) and (21) read

$$\Delta F_2 = -\frac{1}{\beta} \ln\left[\sum_{\nu=1}^{\mathcal{L}} e^{\beta J_1 \sigma_{i_1}\sigma_{i_2}} \Theta[(h_{i_1}^\nu + J_1\sigma_{i_2}^\nu)\sigma_{i_1}^\nu] \Theta[(h_{i_2}^\nu + J_1\sigma_{i_1}^\nu)\sigma_{i_2}^\nu]\right], \tag{31}$$

$$\Delta E_2 = -J_1 \frac{\sum_{\nu=1}^{\mathcal{L}} \sigma_{i_1}\sigma_{i_2} e^{\beta J_1 \sigma_{i_1}\sigma_{i_2}} \Theta[(h_{i_1}^\nu + J_1\sigma_{i_2}^\nu)\sigma_{i_1}^\nu] \Theta[(h_{i_2}^\nu + J_1\sigma_{i_1}^\nu)\sigma_{i_2}^\nu]}{\sum_{\nu=1}^{\mathcal{L}} e^{\beta J_1 \sigma_{i_1}\sigma_{i_2}} \Theta[(h_{i_1}^\nu + J_1\sigma_{i_2}^\nu)\sigma_{i_1}^\nu] \Theta[(h_{i_2}^\nu + J_1\sigma_{i_1}^\nu)\sigma_{i_2}^\nu]}. \tag{32}$$

(iv) Update the population, performing the merging of the branches rooted at $i_1, \ldots, i_k$ onto the site $\Phi = i_{k+2}$: one wants to substitute the $(h_\Phi^\nu, \sigma_\Phi^\nu), \nu = 1, \ldots \mathcal{L}$ with a new population distributed according to $p_\Phi(h,\sigma)$ of Eq. (11). This is the following performed in two steps

(a) First, one makes a list $(\tilde{h}^\nu, \tilde{\sigma}^\nu), \nu = 1, \ldots, \mathcal{L}$ as follows. Start with $\nu = 1$. Enter a loop in which you extract randomly an $\nu' \in \{1, \ldots, \mathcal{L}\}$ and a spin value $\sigma = \pm 1$, until you have the stability condition $\forall j \in \{1, \ldots, k\}, (h_{i_j}^{\nu'} + J_j\sigma)\sigma_{i_j}^{\nu'} \geqslant 0$. Then set $\tilde{h}^\nu = \Sigma_{j=1,\ldots,k} J_j \sigma_{i_j}^{\nu'}$ and $\tilde{\sigma}^\nu = \sigma$. Increment ν, and enter the loop again.

(b) The list $(\tilde{h}^\nu, \tilde{\sigma}^\nu)$ is not the one to overwrite the $(h_\Phi^\nu, \sigma_\Phi^\nu)$ because one must enforce the presence of the factor $e^{\beta h\sigma}$ in Eq. (11). Thus, the elements of the list are to be reweighted: a suitable new population $(h_\Phi^\nu, \sigma_\Phi^\nu), \nu = 1, \ldots, \mathcal{L}$ is obtained by repeating $\mathcal{L}$ times the process of picking an element in the list $(\tilde{h}^\nu, \tilde{\sigma}^\nu), \nu = 1, \ldots, \mathcal{L}$ with a probability proportional to $e^{\beta \tilde{h}^\nu \tilde{\sigma}^\nu}$.

We implemented the above algorithm in the case $k = 2$, using the values $\mathcal{N} = 1000$ and $\mathcal{L} = 1000$. The results are presented in Fig. 8. By contrast with the binary spin glass, the ground state is not degenerated. So both entropies AC and MS go to 0 at the energy density of the ground state E_{GS}. Using the algorithm of Ref. [3] at a low temperature and extrapolating the results to $T = 0$, one finds $E_{GS} = -1.12(1)$, which is compatible with our data [14].

VII. BREAKING THE REPLICA SYMMETRY

Let us now see how our method can be generalized to perform RSB.

A. General considerations

So far, we have assumed there is a single pure state, stable under the iteration process. It is well known that this is actually not true for the spin glass on the Bethe lattice [3]. One should allow for an infinite number of pure states as described by the hierarchical continuous RSB scheme proposed by Parisi [10]. As a first approximation, one can implement the 1RSB scheme. Briefly speaking, one assumes that there exists an infinite number of pure states labeled by $\alpha = 1, \ldots, +\infty$. The free energies of the states on one branch are independent identically distributed random variables, with an exponential density

$$\rho(F) = \exp[\beta x (F - F^R)], \tag{33}$$

where F^R is a reference free energy, and x is Parisi's parameter [10]. In this approach, one computes the average values of the observables as a function of x. The physical value of x is the one which maximizes the free energy.

If one considers a branch rooted at site Φ, in each pure state α, the probability distribution $p_\Phi^\alpha(h,\sigma)$ is different, and the iteration [Eq. (11)] is valid only inside a given pure state. The self-consistency equation to be solved is consequently more complicated than in the replica symmetric case. Let us write $\mathbf{p}_i(h,\sigma) = [p_i^\alpha(h,\sigma)]_{\alpha=1,\ldots}$. One is interested in the set of probability distributions $\mathcal{Q}_\Phi^{(h,\sigma)}(\mathbf{p}) = \overline{\delta(\mathbf{p}_\Phi(h,\sigma) - \mathbf{p})}$, which are functionals of the analogous quantities $\mathcal{Q}_i^{(h,\sigma)}$, and one asks for all of them to be equal. A comprehensive theoretical description of the extension of the cavity method to 1RSB can be found in Ref. [3].

Let us turn to the description of the algorithm. We use a population of $\mathcal{N}$ sites $i = 1, \ldots, \mathcal{N}$, $\mathcal{M}$ states $\alpha = 1, \ldots \mathcal{M}$. On each site, each state is characterized by its own distribution $p_i^\alpha(h,\sigma)$. Depending on the distribution of the coupling

constants, $p_i^\alpha(h,\sigma)$ is represented as a set of $2(k+1)$ numbers (case of binary couplings), or again as a population of $\mathcal{R}$ couples (h,σ) (case of Gaussian couplings).

The RS Algorithm I is nested into the present algorithm: it is used to implement the iteration (11) and compute the expectation values of the observables inside each state. Then a meta-algorithm takes into account all the states, with appropriate weights, to update the population and compute the global expectation values. Two new observables are required with respect to the RS case. First the variation of the free energy during the iteration process described by Eq. (11):

$$\Delta F_{iter} = -\frac{1}{\beta}\ln\left[\operatorname*{Tr}_{\sigma,\sigma_1,\ldots\sigma_k} e^{\beta h_\Phi \sigma}\prod_{i=1}^{k}\int dh_i \Theta[(h_i + J_{\Phi,i}\sigma)\sigma_i] p_i(h_i,\sigma_i)\right]. \tag{34}$$

Second the derivative of the free energy F with respect to x. By derivation of Eqs. (14) and (15), one gets

$$\frac{dF}{dx} = -\frac{F}{x} + d^1 - \frac{k+1}{2}d^2, \tag{35}$$

where

$$d^1 = \frac{1}{x}\frac{\sum_\alpha \Delta F_1^\alpha e^{-\beta x \Delta F_1^\alpha}}{\sum_\alpha e^{-\beta x \Delta F_1^\alpha}}, \tag{36}$$

and similarly for d^2.

An iteration of the algorithm goes as follows:

1. Algorithm III

(i) Perform step (i) of Algorithm I.

(ii) For each state α, perform steps (ii), (iii), and (iv) (computing *en passant* ΔF_{iter}^α), of Algorithm I. One gets quantities bearing α as a superscript: $\Delta F_1^\alpha, \cdots$.

(iii) Reweight the states: this is a crucial step, motivated in Ref. [3]. The states with low ΔF_{iter}^α have to be favored. Thus one picks up $\mathcal{M}$ times an element in the list of distributions $p_\Phi^\alpha, \alpha = 1, \ldots, \mathcal{M}$ with a probability proportional to $\exp(-\beta x \Delta F_{iter}^\alpha)$. The resulting list overwrites the one at site Φ. [Note that the elements one picks up are composite objects, i.e., either a set of $2(k+1)$ numbers or a population of $\mathcal{R}$ couples].

(iv) Compute the global average values of the observables $\Delta F_1, \cdots$. The formulas can be found in Ref. [3]:

$$\Delta F_1 = -\frac{1}{\beta x}\ln\left[\frac{1}{\mathcal{M}}\sum_\alpha e^{-\beta x \Delta F_1^\alpha}\right], \tag{37}$$

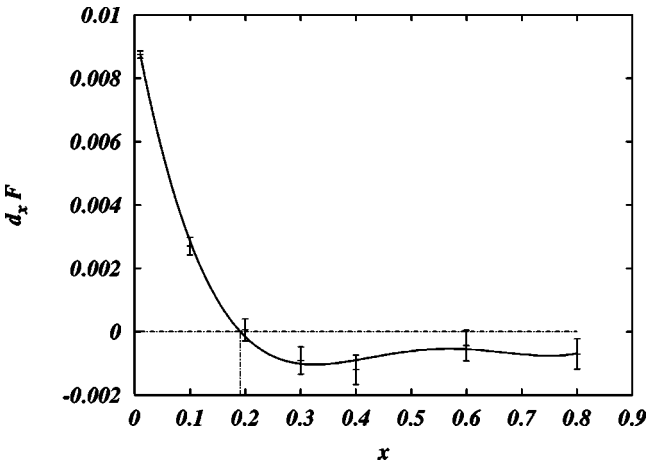

FIG. 9. dF/dx vs x for the binary spin glass in the case $k=2$ at $T=0.5$; the continuous line is the polynomial fit of degree 4.

$$\Delta E_1 = \frac{\sum_\alpha \Delta E_1^\alpha e^{-\beta x \Delta F_1^\alpha}}{\sum_\alpha e^{-\beta x \Delta F_1^\alpha}}, \tag{38}$$

and their obvious analogs for ΔF_2 and ΔE_2. Note that it is essential that the sites and couplings be the same for all the α in step (ii) above.

In practice, we found that the implementation of this algorithm in the case of the Gaussian couplings requires too many computer resources to reach a satisfying accuracy. So we limited ourselves to the case of binary couplings.

B. Application to the binary spin glass

We considered the binary spin glass of Sec. V, at temperature $T=0.5$. Our implementation used the values $\mathcal{N}=1000$ and $\mathcal{M}=1000$. We computed dF/dx for several values of x. The result is presented is Fig. 9. To determine the value x^* of x where dF/dx is zero, we fitted the curve by a polynomial of degree 4, and found its roots. We got $x^*=0.19(1)$. Then we measured the thermodynamic quantities for $x=x^*$, taking into account the uncertainty on x^*:

$$F=-1.280\pm0.001,\quad E=-1.265\pm0.001,$$
$$S=0.029\pm0.001. \tag{39}$$

This is to be compared to the output of the replica symmetric algorithm of Sec. V:

$$F=-1.2816\pm0.0008,\quad E=-1.2685\pm0.0006,$$
$$S=0.0274\pm0.0008. \tag{40}$$

The overall improvement is small, particularly on F. It is more obvious on E and S but still only of the order of 10^{-3}.

VIII. CONCLUSION

In this paper, we have described a general procedure to compute the number of one-spin-flip stable configurations on the Bethe lattice. Given some integer $p \geqslant 2$, the method—at least conceptually—can be easily generalized to compute the number of p-spin-flips stable configurations, i.e., whose energies cannot be decreased by flipping a number of spins ranging from 1 to p. The practical difficulty is that the recursion relations can no longer involve only quantities related to the root of a branch, but must also take into account the $p-1$ successive generations of spins. In the case $p=2$, it remains quite straightforward to write down the equations, but we have not worked out their solution. It might be interesting to do so in order to clarify the nature of the zero temperature limit of the pure states: recently Mézard and Parisi [4] presented a computation at 1RSB level of the number of locally ground states (LGS), i.e., configurations stable with respect to p-spin flips with the number p going to infinity with the size of the system in some unprecised way, and they found some surprising features. There is a need for more precise definitions, and one of the points at issue is how these LGS are related to p-spin flips stable configurations when $p \to +\infty$.

ACKNOWLEDGMENT

We acknowledge very useful discussions with F. Ricci-Tersenghi.

[1] C. De Dominicis and P. Mottishaw, J. Phys. A **20**, L375 (1987).
[2] I. Kanter and H. Sompolinsky, Phys. Rev. Lett. **58**, 164 (1987).
[3] M. Mézard and G. Parisi, Eur. Phys. J. B **20**, 217 (2001).
[4] M. Mézard and G. Parisi, e-print cond-mat/0207121.
[5] G. Biroli and R. Monasson, Europhys. Lett. **50**, 155 (2000).
[6] D.S. Dean, Eur. Phys. J. B **15**, 493 (2000).
[7] A. Lefèvre and D.S. Dean, Eur. Phys. J. B **21**, 121 (2001).
[8] M. Mézard and R. Zecchina, Phys. Rev. E **66**, 056126 (2002).
[9] J. Berg and M. Sellitto, Phys. Rev. E **65**, 016115 (2002).
[10] K. Binder and A.P. Young, Rev. Mod. Phys. **58**, 801 (1986); M. Mézard, G. Parisi, and M.A. Virasoro, *Spin Glass Theory and Beyond* (World Scientific, Singapore 1987); K.H. Fisher and J.A. Hertz, *Spin Glasses* (Cambridge University Press, Cambridge, UK, 1991).
[11] D.J. Aldous, Probab. Th. Related Fields **93**, 507 (1992); Random Struct. Algorithms **18**, 381 (2001).
[12] Marc Mézard and G. Parisi, Europhys. Lett. **3**, 1067 (1987).
[13] S. Boettcher, e-print cond-mat/0208196.
[14] A. Lefèvre and D.S. Dean, J. Phys. A **34**, L213 (2001).